Supporting Information

for

How tailor-made copolymers can control the structure and properties of hybrid nanomaterials: the case of polyionic complexes

Liming Peng[a,b], Maksym Odnoroh[a], Mathias Destarac[a], Yannick Coppel[c], Céline Delmas[d], Florence Benoit-Marquié[a], Christophe Mingotaud[a], Jean-Daniel Marty[a,*]

[a] Laboratoire Softmat, Université de Toulouse, CNRS UMR 5623, 118 route de Narbonne, F-31062 Toulouse, France

[b] Current address: School of Chemistry, Chemical Engineering, and Materials, Jining University, Qufu, Shandong 273155, China

[c] Laboratoire de Chimie de Coordination, Université de Toulouse, CNRS UPR 8241, 205 route de Narbonne, 31062 Toulouse, France

[d] MIAT UR 875, INRAE, Université de Toulouse, F-31326 Castanet-Tolosan, France

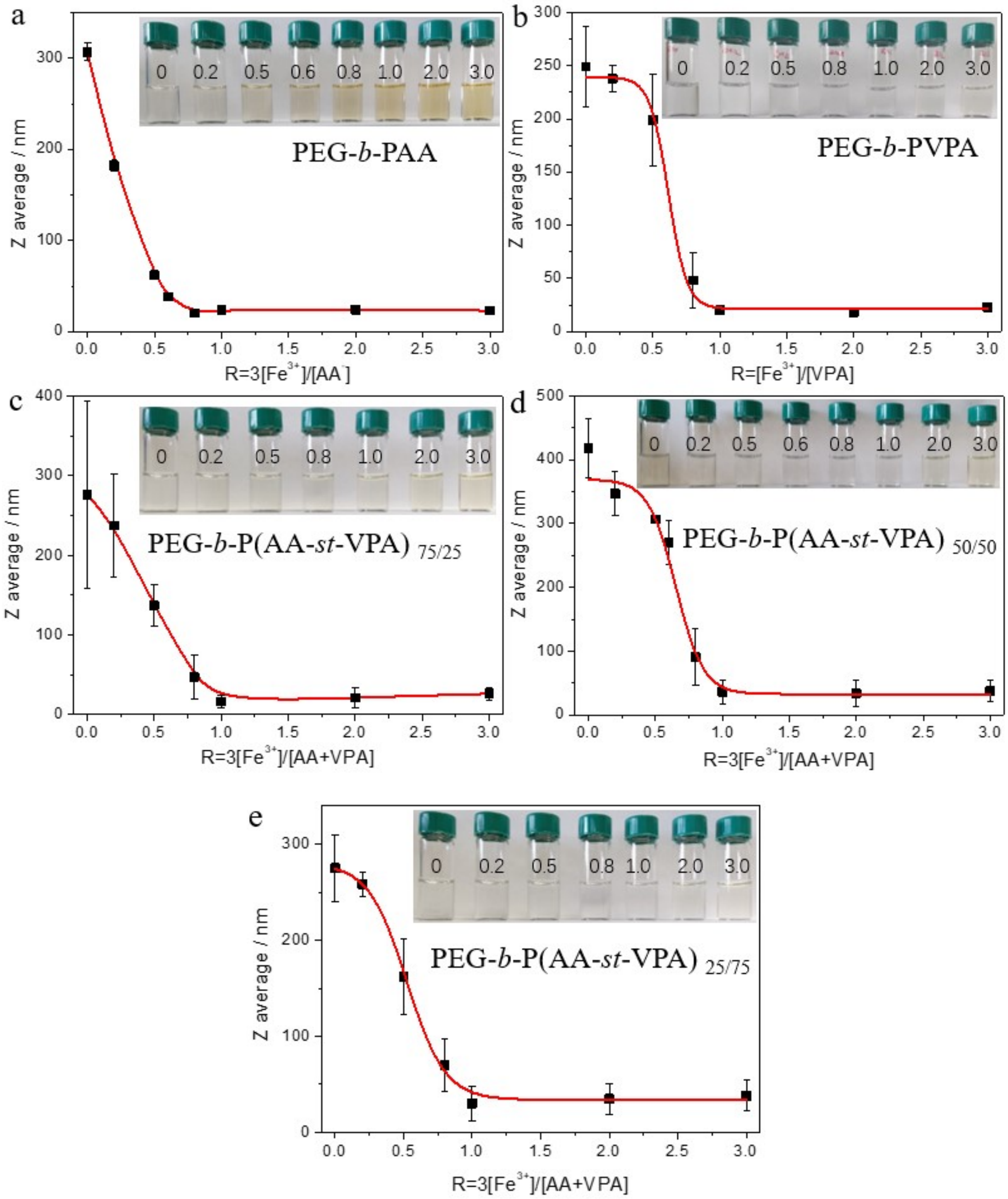

Figure S1. Evolution of the Z-average diameter obtained from DLS measurements of **STHPICs** solutions as a function of R-ratio for Fe^{3+}. The HPICs are based on a) PEG-*b*-PAA, b) PEG-*b*-PVPA, c) PEG-*b*-P(AA-*st*-VPA)$_{75/25}$, d) PEG-*b*-P(AA-*st*-VPA)$_{50/50}$ and e) PEG-*b*-P(AA-*st*-VPA)$_{25/75}$ (with the corresponding pictures).

Table S1. Hydrodynamic size of the **ST-HPICs** synthesized from block copolymers with different PAA/PVPA contents.

ST-HPICs samples	DLS sizes (nm)
HPICs-PAA	24 ± 0.7
HPICs-P(AA-*st*-VPA)$_{75/25}$	16 ± 8.0
HPICs-P(AA-*st*-VPA)$_{50/50}$	36 ± 18
HPICs-P(AA-*st*-VPA)$_{25/75}$	30 ± 18
HPICs-PVPA	20 ± 3.6

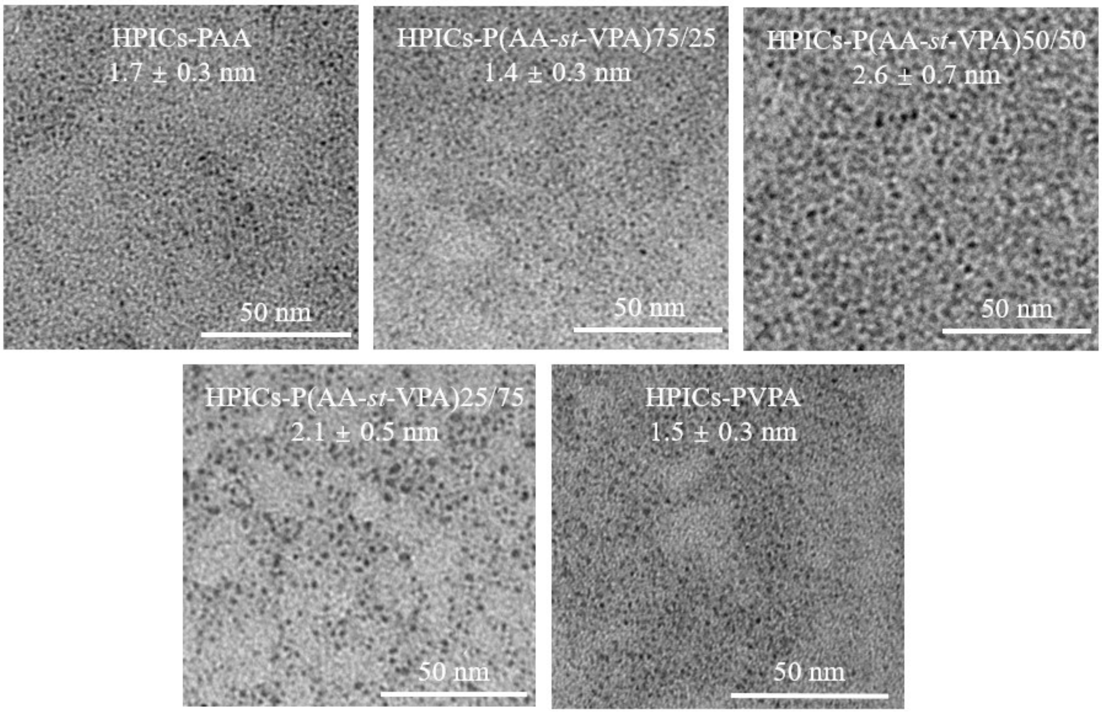

Figure S2. TEM of dried **ST-HPICs** solutions formed by PEG-*b*-P(AA$_x$-*st*-VPA$_{1-x}$) statistical block copolymers.

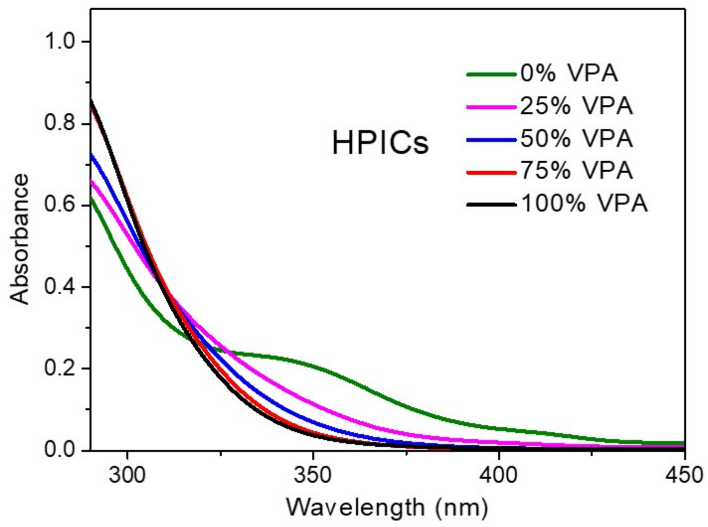

Figure S3. UV-Vis spectra of **ST-HPICs** structures formed by PEG-*b*-P(AA_x-*st*-VPA_{1-x}) statistical block copolymers (pH=3).

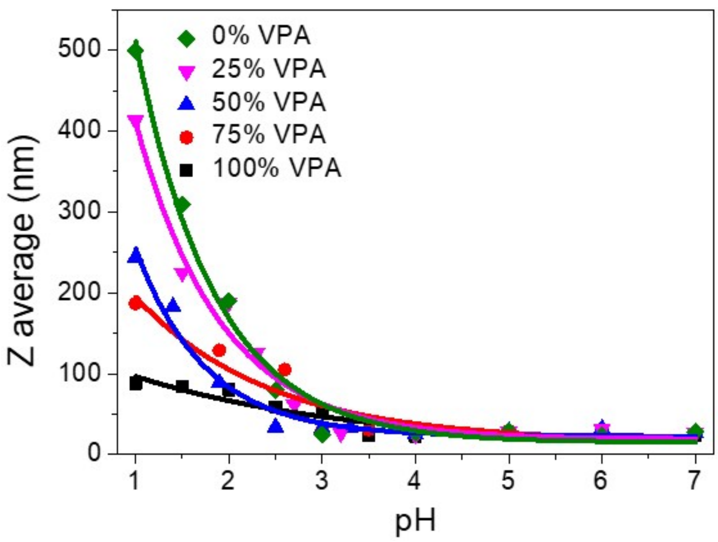

Figure S4. pH stability of **ST** HPICs structures formed by PEG-*b*-P(AA_x-*st*-VPA_{1-x}) statistical block copolymers.

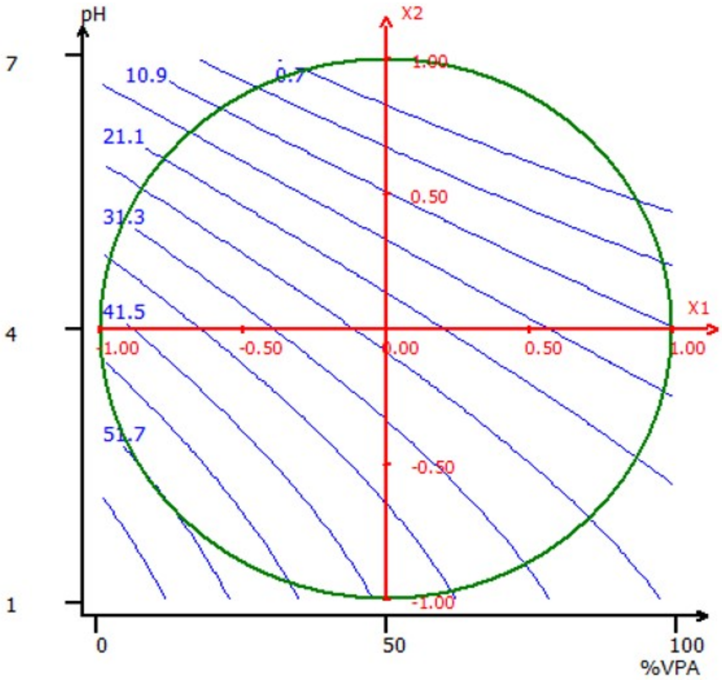

Figure S5. Response surface methodology on the influence of **ST-HPICs** on VPA content and pH. Reaction conditions: **ST-HPICs** HPICs-Fe-R=1.0, $[Fe^{3+}]$= 1.3×10^{-5} M, [AB1]= 2.2×10^{-5} M, $[H_2O_2]$= 1.5×10^{-3} M, reaction time : 2h. x_1 and x_2 represent VPA content and pH respectively.

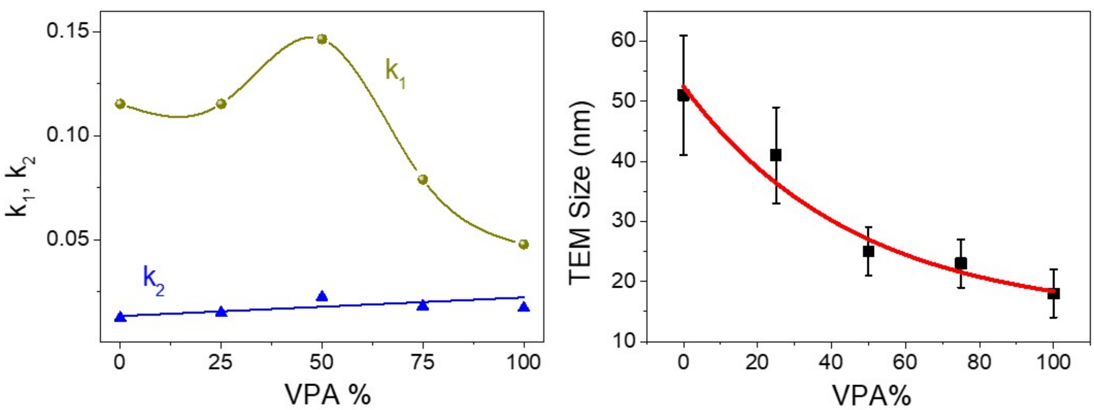

Figure S6. The relationship between VPA content and TEM size of different Prussian blue nanoparticles synthesized with **ST-HPICs** pre-organized system.

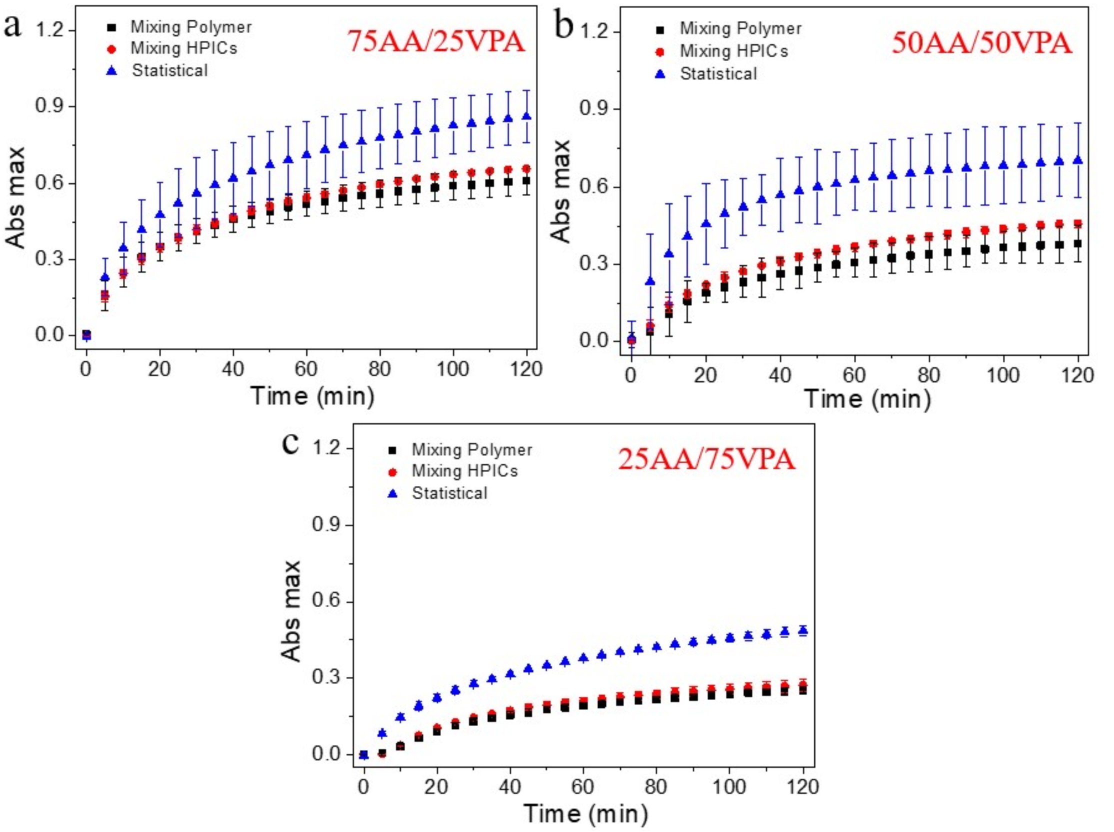

Figure S7. Comparison of the maximum absorbance of Prussian blue nanoparticles generated in real time by three different combinations of HPICs.

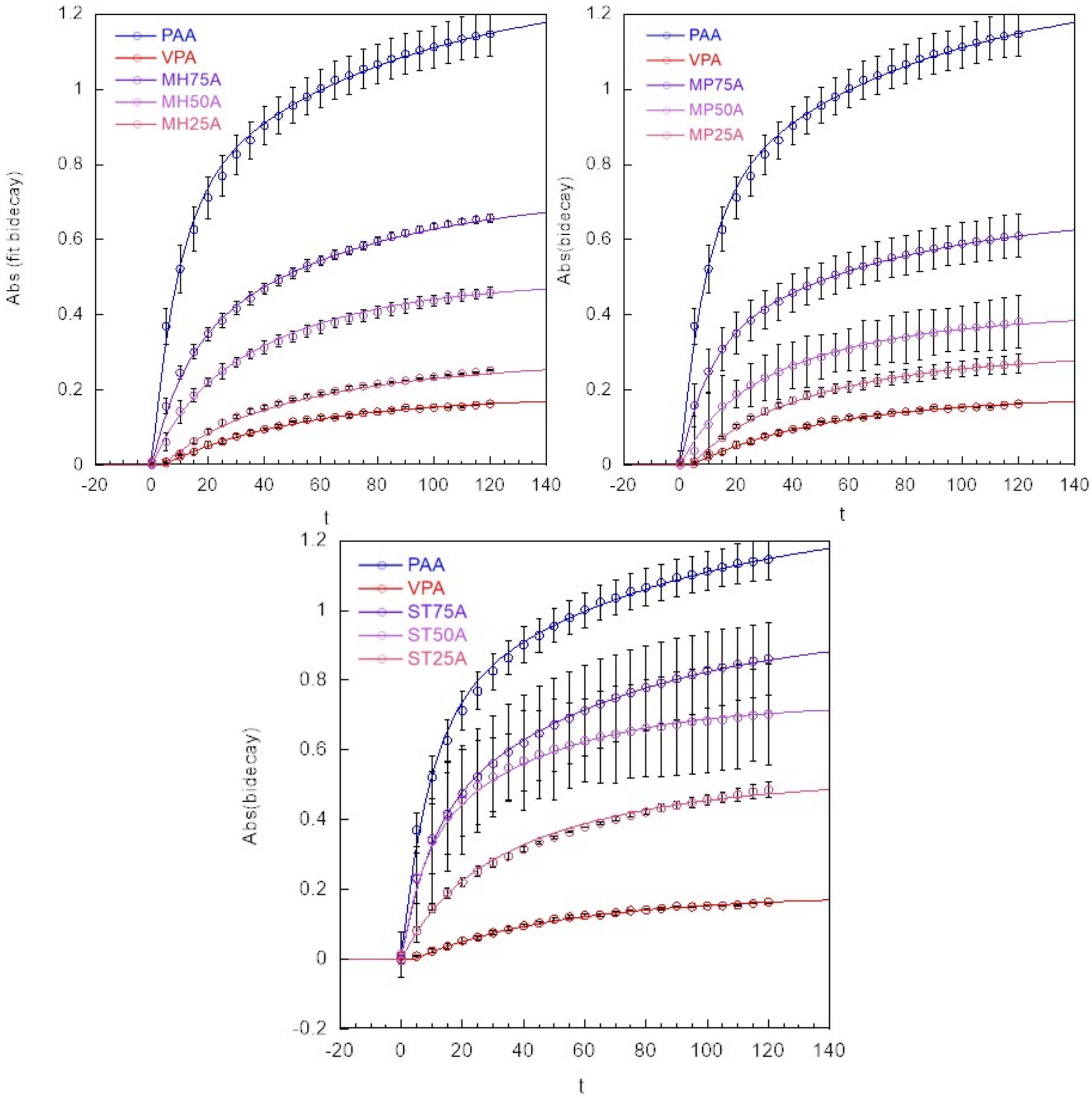

Figure S8. The fitting curve of the maximum absorbance of Prussian blue formed by three different combinations of HPICs (**MH-HPICs**、**MP-HPICs** and **ST-HPICs**).

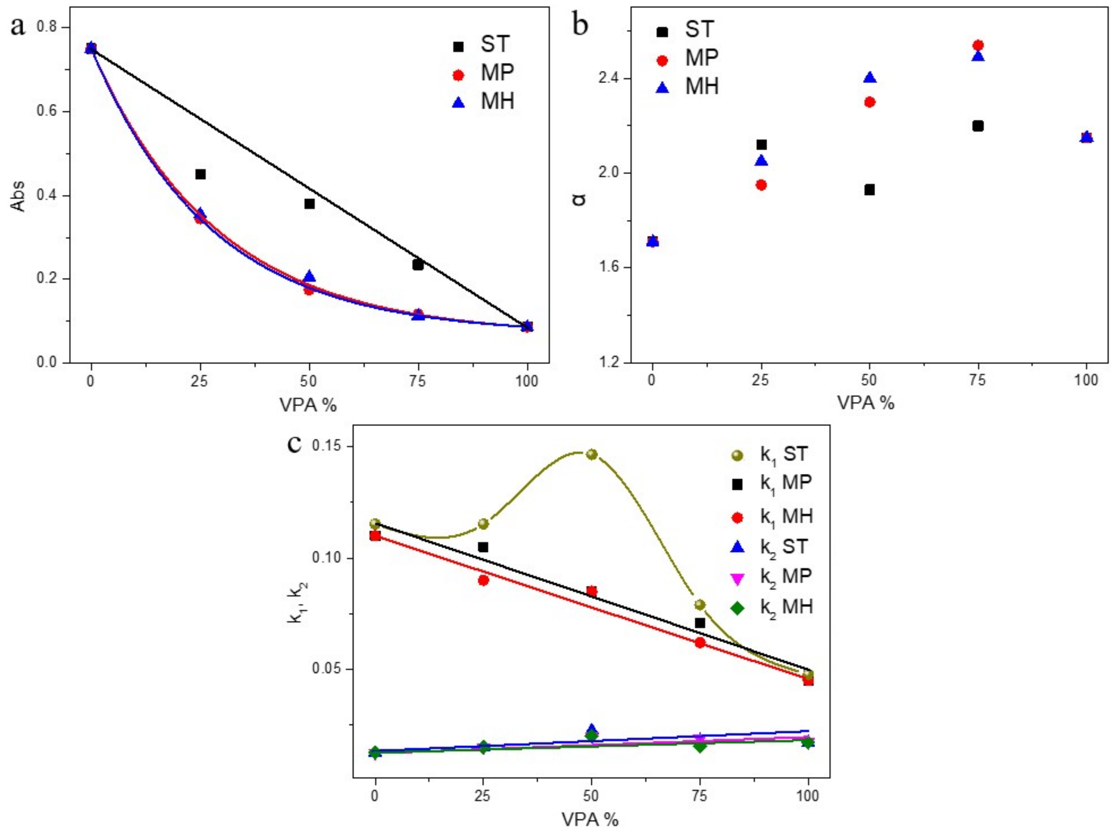

Figure S9. Reaction rate constants k_1 and k_2 versus the content of VPA in the precursor of HPICs for the three types of systems (**ST-HPICs**, **MP-HPICs** and **MH-HPICs**)

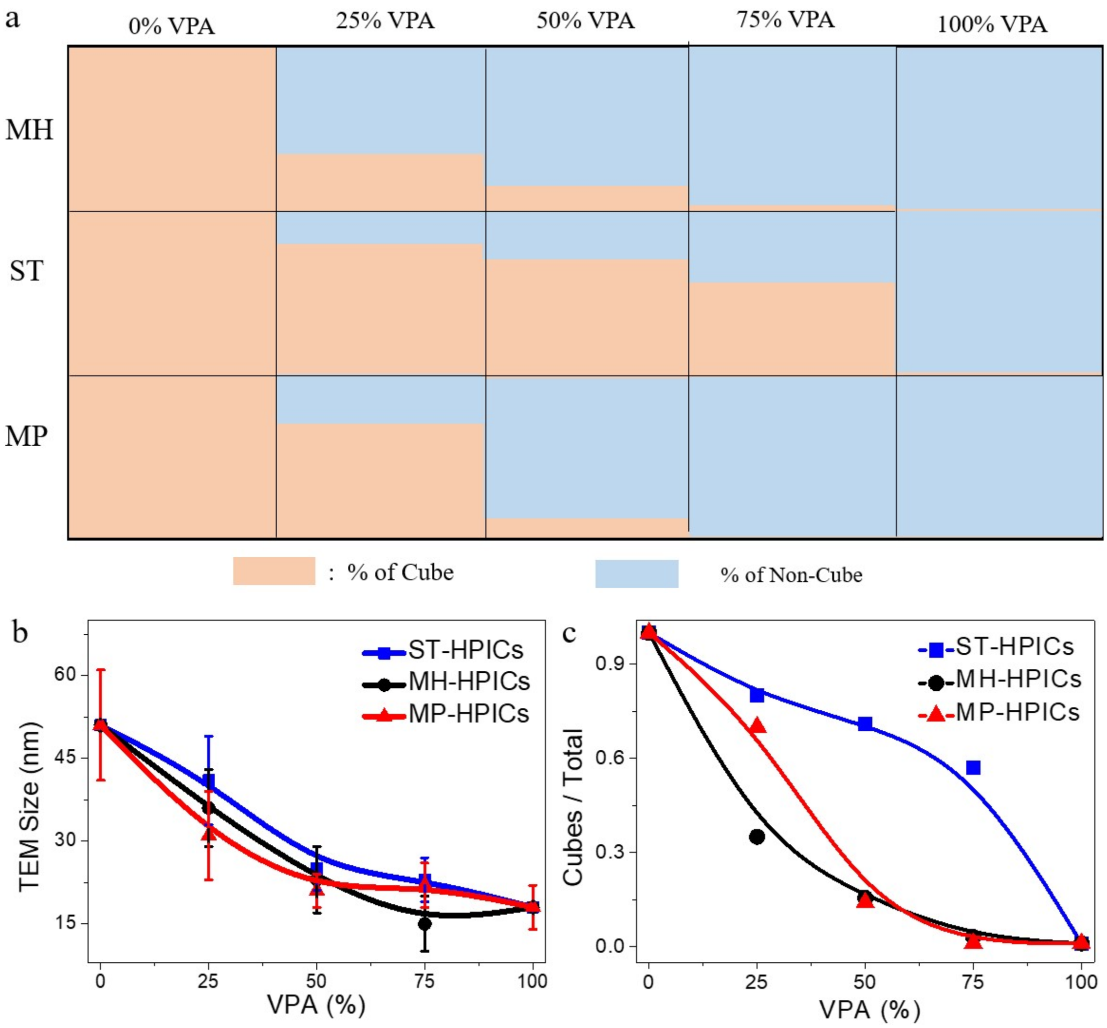

Figure S10. (a) Evolution of the proportion of cubic Prussian blue nanoparticles to total particles synthesized with three different HPICs (**ST**, **MH** and **MP**) as precursors as a function of VPA content. (b) Evolution of TEM size as a function of VPA content for Prussian blue nanoparticles synthesized with HPICs as precursors. (c) Evolution of the proportion of cubic Prussian blue nanoparticles to total particles.

a

Var	PC1	PC2
TEM size (nm)	-0,94	0,20
Ratio cube/total (%)	-0,92	-0,21
Abs	-0,98	0,045
k_1	-0,75	-0,56
k_2	0,51	-0,79
Alpha	0,87	0,14
Degradation ratio at pH3 /(%)	-0,95	-0,01
Degradation ratio at pH1 /(%)	-0,57	-0,71
Release Fe at pH3 (%)	-0,90	0,35
Release Fe at pH1 (%)	-0,97	0,20

b

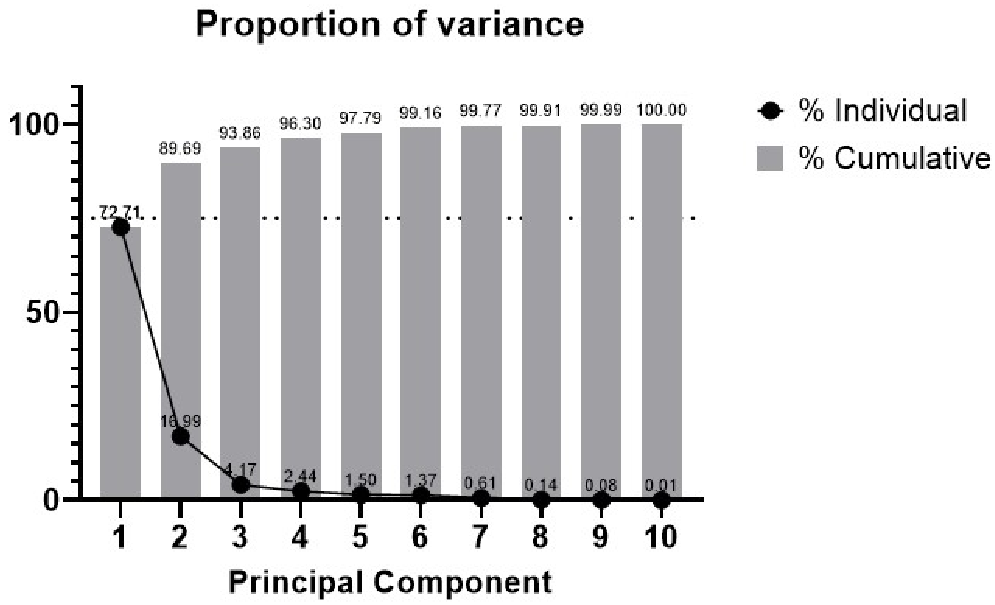

Figure S11. (a) Correlation between principal components PC1 and PC2 and experimental data (b) Proportion of variance (individual and cumulative) of calculated principal components.

Table S2. Data use for multivariate analysis.

	Type of system	%AA	TEM size(nm)	Standard deviation(nm)	Ratio cube/total (%)	Abs	k_1	k_2	Alpha	Degradation ratio at pH3 /(%)	Standard deviation-pH3/(%)	Degradation ratio at pH1 /(%)	Standard deviation-pH1/(%)	Release Fe at pH3 (%)	Release Fe at pH1 (%)
100/0	ST	100	51	10	100	0.75	0.11	0.0125	1.71	84.5	8.5	31.5	0.4	26	77
75/25	ST	75	41	8	80	0.45	0.11	0.015	2.12	63.5	3.6	31	1.6	12	40
50/50	ST	50	25	4	71	0.38	0.14	0.0225	1.93	48	7.3	36.5	6.9	6	24
25/75	ST	25	23	4	57	0.235	0.075	0.018	2.2	16	3.2	35	2.4	4.5	11
0/100	ST	0	18	4	1	0.0867	0.045	0.0172	2.15	4.35	0.5	26.5	3.7	3	4.5
75/25	MH	75	36	7	35	0.355	0.09	0.015	2.05	58	2.4	34	4.9	9.4	30
50/50	MH	50	23	6	15.5	0.205	0.085	0.02	2.4	36	2.4	32.5	4.7	6	15
25/75	MH	25	15	5	3	0.113	0.062	0.0156	2.49	16	2.4	23	5.7	4.2	7
75/25	MP	75	31	8	70	0.345	0.105	0.015	1.95	69.5	4.5	35.5	2	10.6	37
50/50	MP	50	21	3	14	0.175	0.085	0.018	2.3	27	4.8	29.5	1.2	7.3	17
25/75	MP	25	22	4	1	0.117	0.071	0.019	2.54	18.5	2	26	2.4	5.2	6.2

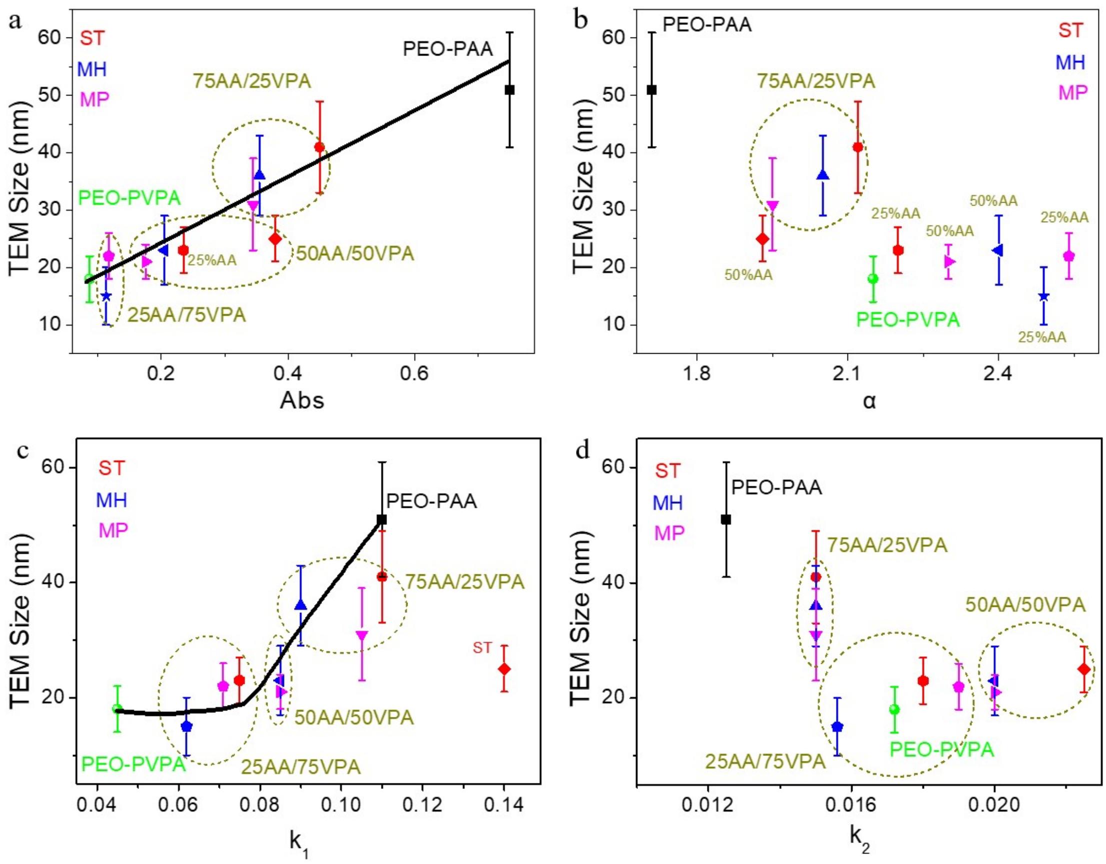

Figure S12. Relationship between TEM size of Prussian blue nanoparticles synthesized using three different polyions complexes (**MP**, **MH**, and **ST**) as precursor materials and the kinetic data during their formation: (a) max absorbance; (b) α; (c) k_1 and (d) k_2.

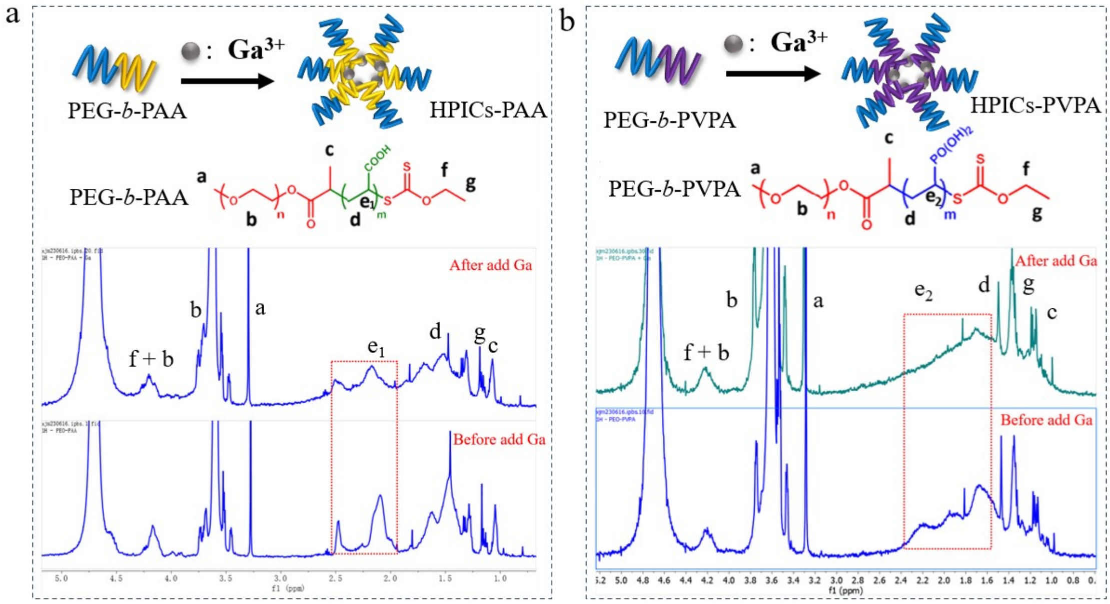

Figure S13. (a) ^{1}H NMR spectra of the double hydrophilic block copolymer PEG-*b*-PAA before and after binding with gallium (Ga^{3+}) ions (including hypothetical schematic diagram). (b) ^{1}H NMR spectra of the double hydrophilic block copolymer PEG-*b*-PVPA before and after binding with gallium (Ga^{3+}) ions (including hypothetical schematic diagram).